

Supporting Information

Photo-Cross-Linked Self-Assembled Poly(Ethylene Oxide) Based Hydrogels Containing Hybrid Junctions with Dynamic and Permanent Crosslinks

Erwan Nicol^{a,}, Taco Nicolai^a, Jingwen Zhao^b, Tetsuharu Narita^{b,c}*

^a IMMM – UMR CNRS 6283, Le Mans Université, avenue O. Messiaen, 72085 Le Mans cedex 9, France

^b Laboratoire Sciences et Ingénierie de la Matière Molle, ESPCI Paris, PSL University, Sorbonne Université, CNRS, 75005 Paris, France

^c Global Station for Soft Matter, Global Institution for Collaborative Research and Education, Hokkaido University, Sapporo, Japan

CONTENTS

Materials and methods:

Block copolymer synthesis and characterization	P. 3
Figure S1	P. 4
Sample preparation	P. 4
Experimental methods	P. 5
Structure of tPEO/IEI mixtures	P. 6
Figure S2	P. 7
Figure S3	P. 7
Rheological properties of tPEO/IEI mixtures before photo-cross-linking	P. 8

Figure S4	P. 8
Figure S5	P. 9
Figure S6	P. 10
Photo-cross-linked hybrid covalent/dynamic hydrogels	P. 11
Figure S7	P. 11
Figure S8	P. 11
Figure S9	P. 12
Figure S10	P. 12
Figure S11	P. 13
Figure S12	P. 13
References	P. 14

Materials and Methods

Block copolymers synthesis

Amphiphilic triblock copolymers were synthesized according to already published procedures¹⁻⁴. Briefly, a triple hydrophilic poly(2-hydroxyethyl acrylate)-b-poly(ethylene oxide)-b-poly(2-hydroxyethyl acrylate), PHEA-b-PEO-b-PHEA, was synthesized by growing two PHEA blocks from a dibrominated PEO (Br-PEO-Br) macroinitiator using SARA-ATRP. In the case of PEO_{12k} of $M_n=12\ 000$ g/mol, the synthesis was performed in DMSO³ with a molar ratio [Br-PEO-Br]/[HEA]/[Me₆TREN]/[CuBr₂] : 1/8/0.2/0.05. Copper wire was used as a catalyst. Prior to use the copper surface was activated with sulfuric acid. A degree of polymerization of 7 for the PHEA blocks was obtained at 90% conversion. In the case of PEO_{35k} of $M_n=35\ 000$ g/mol, the synthesis was performed in water⁴ with a molar ratio [Br-PEO-Br]/[HEA]/[Me₆TREN]/[CuBr]/[CuBr₂] : 1/10/0.5/0.3/0.2. A degree of polymerization of 9 for the PHEA blocks was obtained at 90% conversion. Polymerizable methacrylate functions were then grafted onto the PHEA-blocks leading to the UV-crosslinkable hydrophobic poly(methacryloyloxyethyl acrylate) (PMEA) blocks. ¹H NMR analysis of both final PMEA-b-PEO-b-PMEA (tPEO) triblock copolymers indicated a quantitative functionalization of the HEA units into methacryloyloxyethyl acrylate ones. The number (M_n) and weight (M_w) average molar mass and dispersity ($\mathcal{D}=M_w/M_n$) were determined by Size Exclusion Chromatography (SEC) in THF using light scattering and refractometric detection. $M_n=1.42\times 10^4$ g/mol, $M_w=1.59\times 10^4$ g/mol, $\mathcal{D}=1.1$ were measured for tPEO_{12k}. $M_n=4.21\times 10^4$ g/mol, $M_w=5.53\times 10^4$ g/mol, $\mathcal{D}=1.3$ were measured for tPEO_{35k}.

Poly(isobutyryloxyethyl acrylate)-b-poly(ethylene oxide)-b-poly(isobutyryloxyethyl acrylate) (PIEA-b-PEO-b-PIEA: IEI) was synthesized by esterification of PHEA-b-PEO_{12k}-b-PHEA with isobutyryl chloride in the presence of triethylamine and DMPA using the same procedure as that used for synthesizing PMEA-b-PEO-b-PMEA^{1,5}. ¹H NMR analysis of the resulting IEI triblock copolymer indicated 85% of functionalization of the HEA units into isobutyryloxyethyl acrylate ones (Figure S1). The hydrophobic block was thus a statistical copolymer poly((isobutyryloxyethyl acrylate)_{0.85}-co-(2-hydroxyethyl acrylate)_{0.15}). $M_n=1.42\times 10^4$ g/mol, $M_w=1.59\times 10^4$ g/mol, $\mathcal{D}=1.1$ were measured by multi-detection SEC.

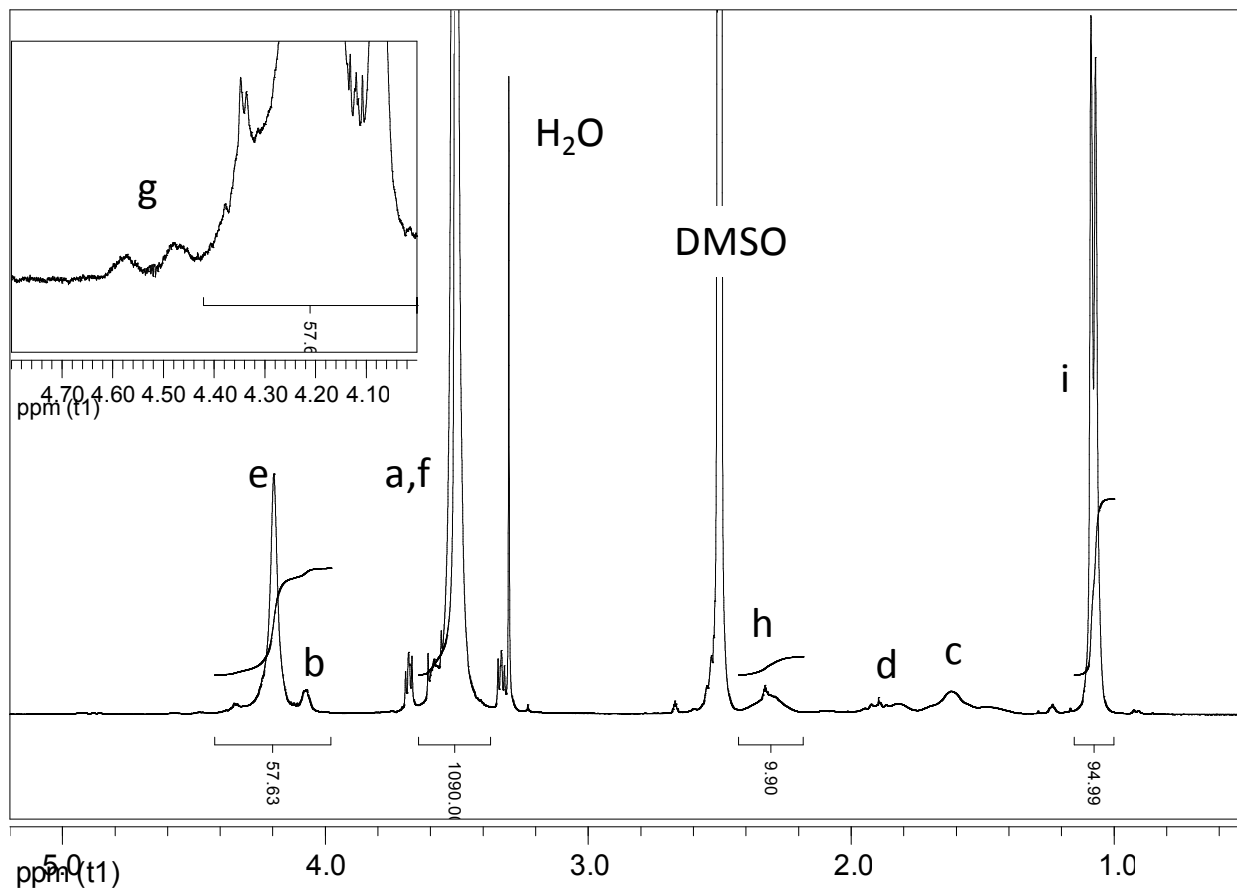
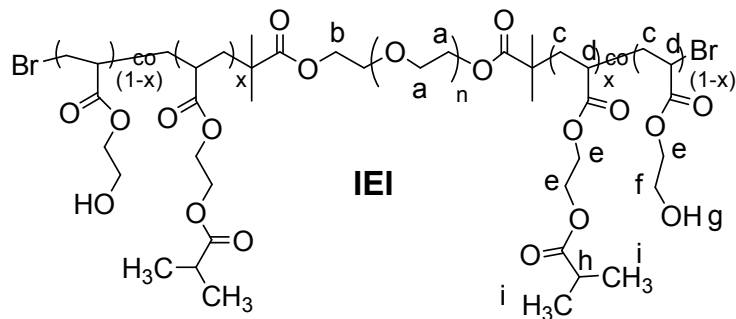


Figure S1. ^1H NMR of PIEA-*b*-PEO-*b*-PIEA (IEI) copolymer in DMSO- d_6 ($\nu_0=400$ MHz)

Sample preparation

Stock solutions of tPEO were prepared by dissolving the polymer powder in deionized water (MilliPore) and stored at 4 °C. For photo-cross-linking experiments a solution of 2,2-dimethoxy-2-phenylacetophenone (DMPA) photoinitiator (0.01 M) was prepared in THF. The required amount of solution of DMPA was placed on the walls of a glass vial, and THF was evaporated under a gentle flow of argon. Then, the polymer dissolved in deionized Milli-Q water was

introduced into a vial that was sealed with a rubber septum. The vial was rotated overnight on a roller stirrer. The quantity of DMPA was fixed to around 10 molecules per micelle considering the average aggregation number determined below.

Methods

Oscillatory shear measurements were done with a stress-controlled rheometer MCR-301 (Anton Paar) equipped with a cone and plate geometry (gap 0.103 mm, diameter 25 mm). For in-situ cross-linking, the samples were degassed in advance and introduced into the rheometer under gentle flow of argon. In order to prevent evaporation, the geometry was covered with silicon oil. The samples were irradiated by a UV light (Dymax Bluewave-200 lamp) at 365nm under air with an intensity 0.17 W.cm^{-1} during 60 s. The measurements were done in the linear response regime unless otherwise specified.

Static and dynamic light scattering measurements were done using a commercial static and dynamic light scattering equipment (ALV-Langen, Germany and LS-Instruments, Switzerland) operating with a vertically polarized laser with wavelength $\lambda=632 \text{ nm}$. The measured scattered light intensity was corrected for that of the solvent and normalized by that of toluene. The relative excess scattering intensity (I_r) was multiplied with the Rayleigh factor of toluene and expressed in units of cm^{-1} . The measurements were done at $20 \text{ }^\circ\text{C}$ using a thermostated bath over a range of scattering wave vectors ($q=4.\pi.n.\sin(\theta/2)/\lambda$), with θ the angle of observation and n the refractive index of the solvent). The electric field autocorrelation function ($g_1(t)$) was calculated from the normalized intensity autocorrelation functions ($g_2(t)$): $g_2(t)=1+g_1(t)^2$ and was analyzed in terms of a relaxation time distribution:

$$g_1(t) = \int A(\log \tau) \exp(-t / \tau) d \log \tau \quad (1)$$

At low polymer concentration a single relaxation mode was observed, but at higher concentrations a second slower and broader relaxation mode was observed. All correlation functions could be well-described using a log-normal distribution for the fast mode and a generalized exponential for the slow mode:

$$A(\log \tau) = k \tau^p \exp\left[-\left(\tau / \tau^*\right)^s\right] \quad (2)$$

The average relaxation rates ($\Gamma = \langle \tau^{-1} \rangle$) of the single mode at low concentrations and of the fast mode at high concentrations were found to be q^2 -dependent and the cooperative diffusion coefficient was calculated as

$$D_c = \Gamma \cdot q^{-2}$$

The large deformation behavior of the gels was studied by uniaxial tensile and loading–unloading tests on an Instron 5565 tensile tester with a 10 N load cell. Samples were rectangular in shape with 5 mm width, 3 mm thickness, and 20 mm length (length between clamps). We kept the samples in paraffin oil during all the tests to prevent them from drying.

Structure of tPEO/IEI mixtures

The structure of self-assemblies formed by PMEA-b-PEO-b-PMEA (tPEO) and PIEA-b-PEO-b-PIEA (IEI) triblock copolymers were studied individually and in mixtures. The apparent molar mass (M_a) and hydrodynamic radius (R_{ha}) of individual tPEO_{12k} and IEI aggregates were obtained by static and dynamic light scattering as described in the materials and methods section and are shown as a function of the polymer concentration in Figure S2. As was already reported observed for similar systems in the literature^{2,6} M_a and R_{ha} increased with increasing concentration due to the bridging of micelles leading to formation of larger aggregates. At high concentrations, M_a decreased because repulsive interactions dominated⁶. The number of hydrophobic blocks per micellar core (N_{agg}) could be estimated from M_a measured at 1 g/L, because at this concentration, repulsive interactions between micelles were negligible and micelles were mainly in the form of single flowers¹. $N_{agg} \approx 60$ was found for tPEO_{12k} micelles and $N_{agg} \approx 30$ for IEI_{12k} micelles. The large difference between tPEO and IEI is probably due to the lower hydrophobicity of the PIEA blocks which contained about 15% residual hydrophilic units whereas PMEA blocks did not. N_{agg} of tPEO_{35k} was also approximately 30 (Figure S3).

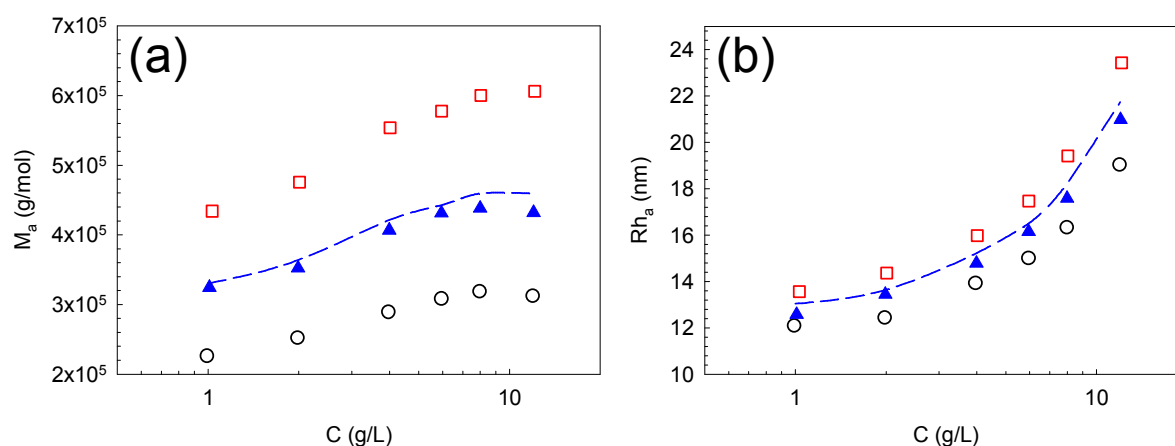


Figure S2. Concentration dependences of **(a)** the apparent molar mass (M_a) and **(b)** the apparent hydrodynamic radius (Rh_a) for the IEI aggregates (open circles), tPEO_{12k} (open squares) and tPEO_{12k}/IEI 50/50 (%v/v) mixtures (filled triangles). Blue dashed lines represent the theoretical evolution of non-hybridizing aggregates mixture (equation (3) and (4)).

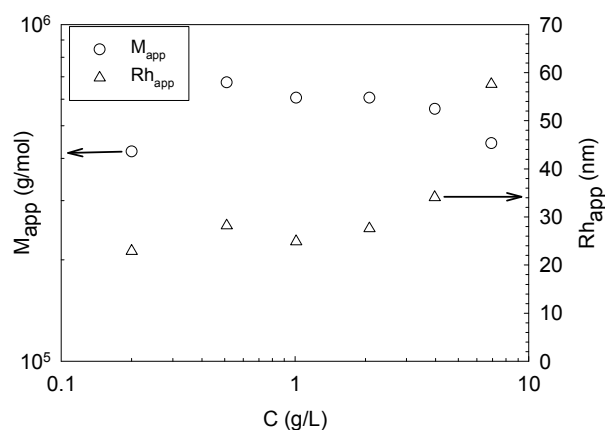


Figure S3. Concentration dependence of the apparent molar mass and apparent hydrodynamic radius of tPEO_{35k} aggregates in water.

The concentration dependences of M_a and Rh_a of tPEO_{12k}/IEI 50/50 (vol/vol) mixtures are also shown in Figure S2. Note that all the mixtures formed homogenous transparent solutions. The same qualitative dependence was observed for the mixture and the individual systems. The

experimental data were compared with calculated values of M_a (weight-averaged) and Rh_a (z-averaged) considering no interaction between tPEO_{12k} and IEI in the mixture:

$$M_a(mix) = \frac{M_a(tPEO).C(tPEO)+M_a(IEI).C(IEI)}{C(tPEO)+C(IEI)} \quad (3)$$

$$Rh_a(mix) = \left[\frac{M_a(tPEO).C(tPEO).[Rh_a(tPEO)]^{-1}+M_a(IEI).C(IEI).[Rh_a(IEI)]^{-1}}{M_a(tPEO).C(tPEO)+M_a(IEI).C(IEI)} \right]^{-1} \quad (4)$$

The calculated values are close to the experimental data at low polymer concentrations where the effect of interaction is small. This suggests that either hybridization did not occur or that N_{agg} of the hybrid micelles was the same as the calculated average.

Rheological properties of tPEO/IEI mixtures before photo-cross-linking

The viscosity of individual systems and mixtures was measured as function of the shear rate. All solutions exhibited Newtonian behavior over large range of shear rates, but the most viscous solutions showed shear thinning at shear rates above 10 s⁻¹ (see Fig S4a and S4b).

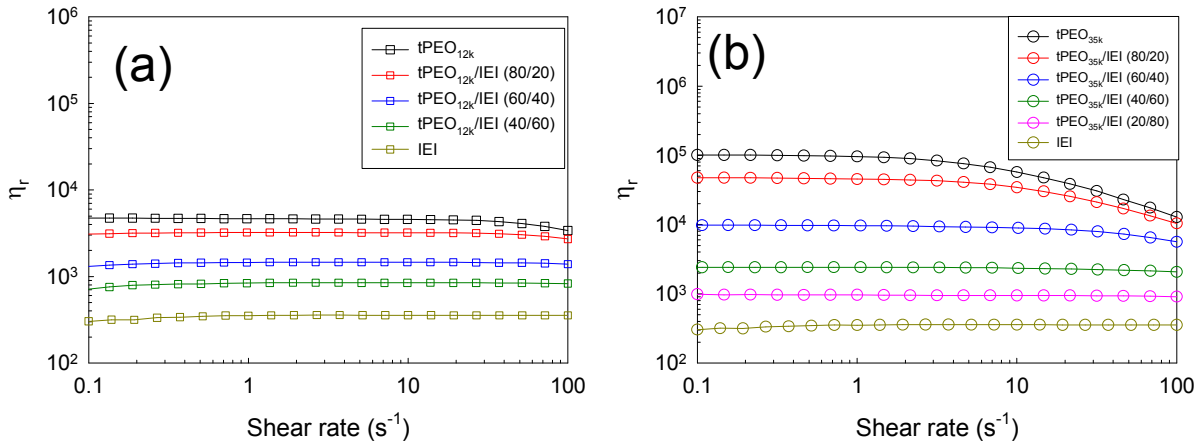


Figure S4. Shear rate dependence of the relative viscosity of **(a)** tPEO_{12k}/IEI hybrid hydrogels at $C=50 \text{ g.L}^{-1}$ and **(b)** tPEO_{35k}/IEI hybrid hydrogels at $C=50 \text{ g.L}^{-1}$

Individual triblock copolymer solutions showed a strong increase of the relative zero-shear viscosity (η_r) with increasing concentration above a critical value (C_p) (Figure S5a). The strong increase of η_r was caused by formation of a transient network of bridged micelles and C_p

corresponds to the percolation threshold. We found $C_p \approx 15$ g/L for tPEO_{12k} and IEI and $C_p \approx 8$ g/L for tPEO_{35k}.

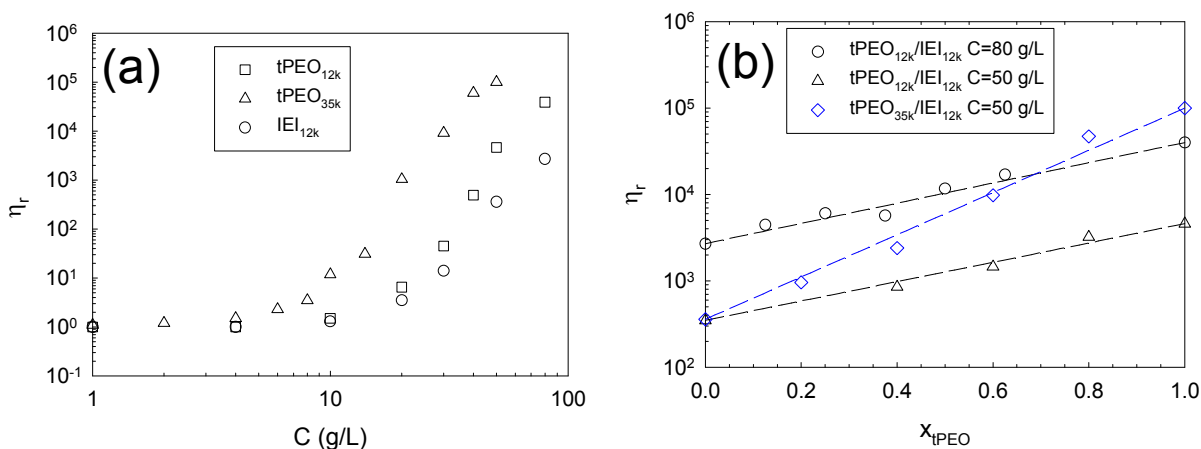


Figure S5. (a) Concentration dependence of the relative viscosity of IEI_{12k}, tPEO_{12k} and tPEO_{35k} at $T=20$ °C. **(b)** Evolution of the relative viscosity with the weight fraction of tPEO in tPEO/IEI mixtures at various concentrations. Dashed lines are fits to equation (5).

The viscosity of tPEO_{12k}/IEI and tPEO_{35k}/IEI mixtures was measured as a function of the composition $C = 50$ g/L. In addition, tPEO_{12k}/IEI mixtures were studied at $C = 80$ g/L. The dependence of η_r on the weight fraction of tPEO (x) in the mixtures is shown in Fig. S5b. Interestingly, for a given C , η_r had a logarithmic dependence on x :

$$\log(\eta_{r(hyb)}) = x_{tPEO} \cdot \log(\eta_{r(tPEO)}) + x_{IEI} \cdot \log(\eta_{r(IEI)}) \quad (5)$$

This behavior noticeably differs from that exhibited by mixtures of other types of self-assembled triblock copolymers^{7,8}. In the case of hydrophobically end-capped PEO, Annable et al.⁷ reported that chains with different end-cap alkyl lengths relaxed independently. This implies that the viscosity of the mixtures was governed by the polymers with the longest relaxation time, i.e. the highest viscosity. In the case of mixtures of pH-sensitive amphiphilic triblock copolyelectrolytes the viscosity was also governed by that of the most viscous copolymer as soon as it formed a percolated network⁸. In this latter case, although the evolution of the viscosity was not strictly proportional to the evolution of the mean relaxation time τ (lifetime of a hydrophobic block in a micellar core), it followed the same tendency.

The frequency dependence of the shear moduli was determined as a function of x . It showed a single relaxation mode that shifted to lower frequencies with increasing x , see Fig. S6.

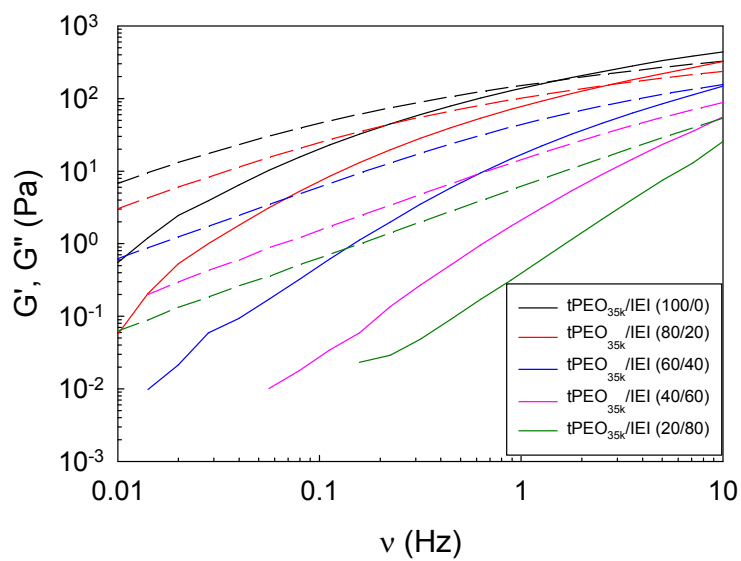


Figure S6. Frequency dependences of the storage (G') and loss (G'') moduli of tPEO_{35k}/IEI mixtures at $C_{\text{tot}}=50$ g/L and $T=20$ °C.

Photo-cross-linked hybrid covalent/dynamic hydrogels

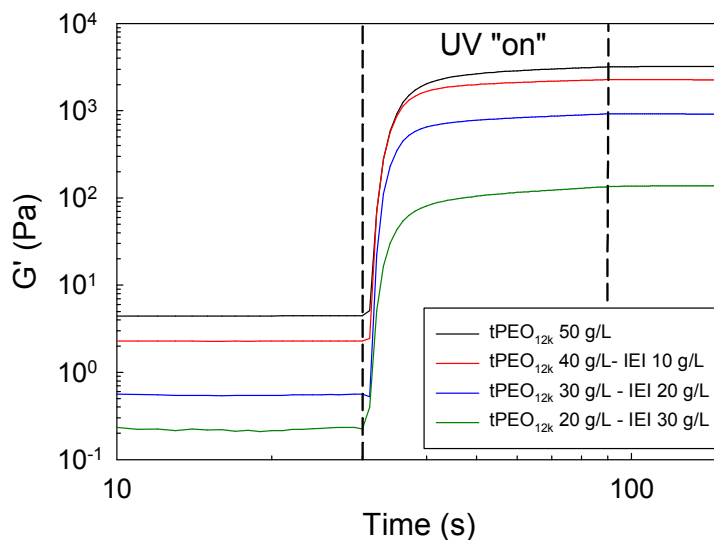


Figure S7. Evolution of the elastic modulus (G') during the photo-cross-linking step of tPEO_{12k}/IEI hybrid hydrogels at constant polymer concentration $C = 50$ g/L ($\gamma=2$ %, $f=1$ Hz)

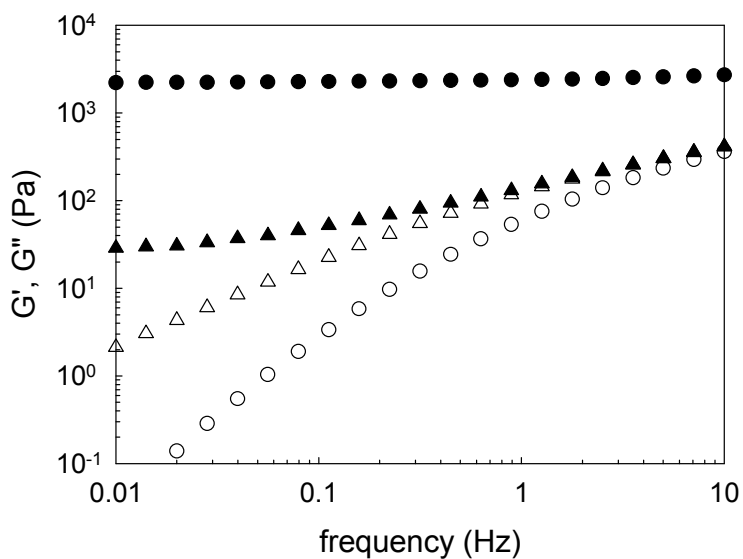


Figure S8. Frequency dependence of the storage (G' , circles) and loss (G'' , triangles) moduli before (open symbols) and after UV-irradiation (filled symbols) of tPEO_{35k}/IEI (40 g/L-40 g/L) mixture

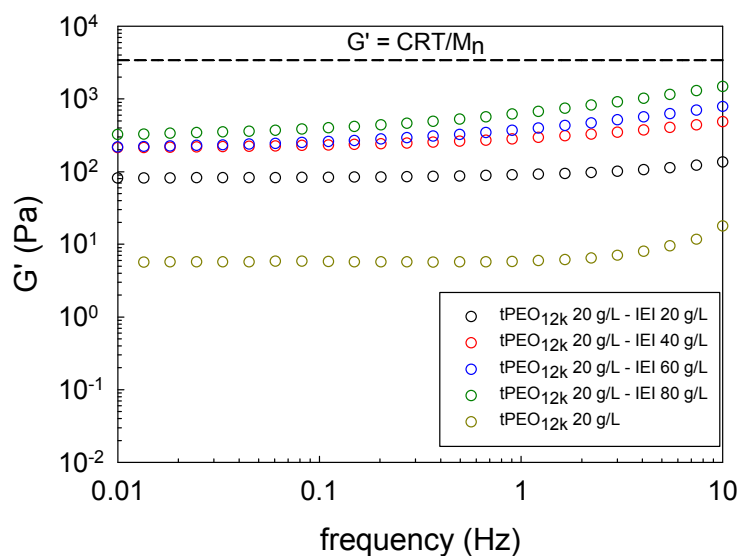


Figure S9. Frequency dependence of the storage modulus of photo-cross-linked hybrid tPEO_{12k}/IEI for $C_{\text{tPEO}_{12k}}=20$ g/L and various concentration of IEI. The dashed line corresponds to the theoretical value of G' using the affine model assuming that all the tPEO_{12k} chains are elastically active.

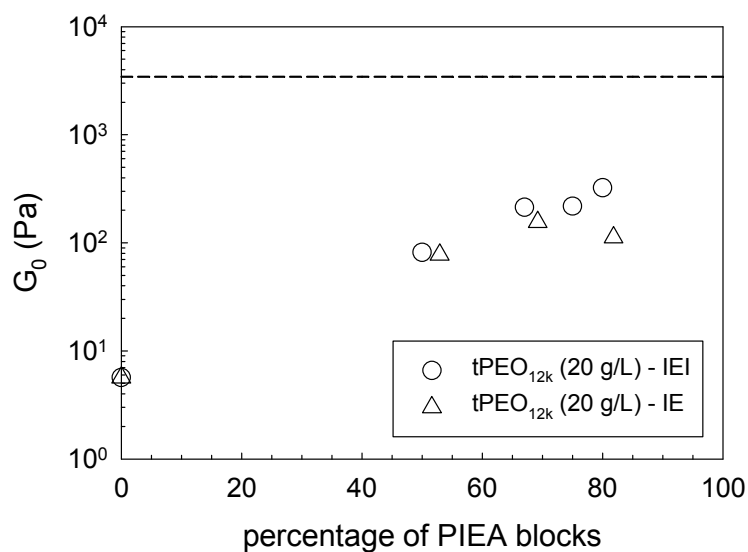


Figure S10. Evolution of the low frequency storage modulus (measured at 0.01 Hz) as a function of the molar percentage of PIEA blocks in the micelle cores for tPEO_{12k} ($C=20$ g/L) mixed with IEI triblock copolymer (circles) or IE diblock copolymer (triangle)

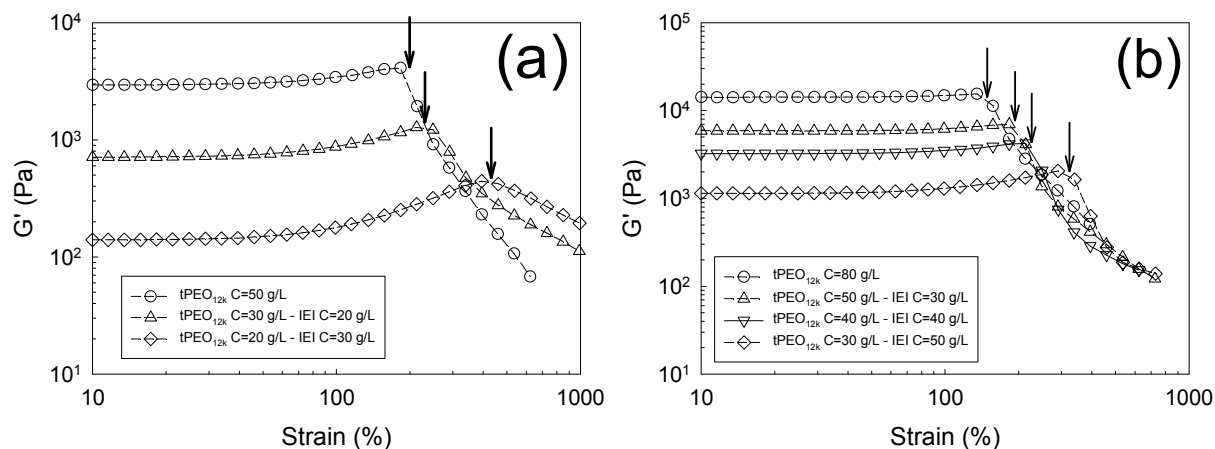


Figure S11. Strain dependence of the elastic modulus (G') for tPEO_{12k}/IEI hybrid photo-cross-linked hydrogels at total polymer concentration (a) $C=50$ g/L and (b) $C=80$ g/L and varying the tPEO_{12k}/IEI ratio.

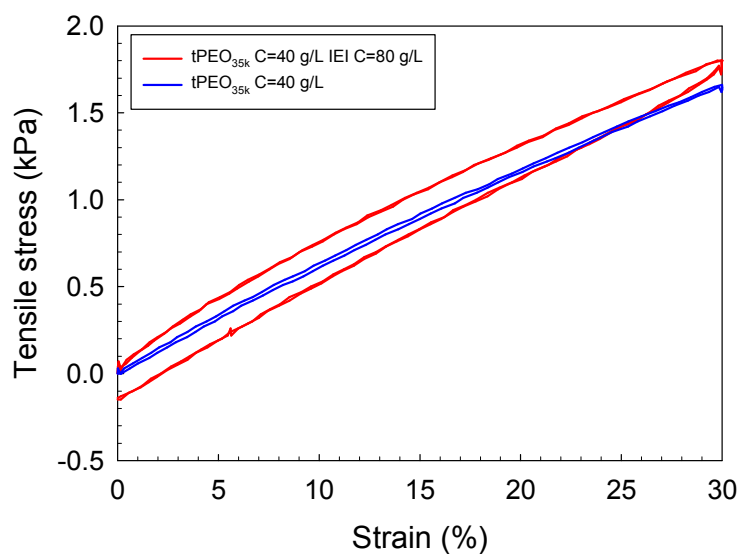


Figure S12. Evolution of the tensile stress with strain during cyclic loading-unloading experiments.

References

- (1) Kadam, V. S.; Nicol, E.; Gaillard, C. *Macromolecules* **2012**, *45*, 410-419.
- (2) Klymenko, A.; Nicolai, T.; Benyahia, L.; Chassenieux, C.; Colombani, O.; Nicol, E. *Macromolecules* **2014**, *47*, 8386-8393.
- (3) Nicol, E.; Derouineau, T.; Puaud, F.; Zaitsev, A. *Journal of Polymer Science Part A: Polymer Chemistry* **2012**, *50*, 3885-3894.
- (4) Nicol, E.; Nzé, R.-P. *Macromolecular Chemistry and Physics* **2015**, *216*, 1405-1414.
- (5) Piogé, S.; Fontaine, L.; Soutif, J.-C.; Nicol, E.; Pascual, S. *J. Pol. Sci. Part A: Pol. Chem.* **2010**, *48*, 1526-1537.
- (6) Kadam, V.; Nicolai, T.; Nicol, E.; Benyahia, L. *Macromolecules* **2011**, *44*, 8225-8232.
- (7) Annable, T.; Buscall, R.; Ettelaie, R.; Whittlestone, D. *J. Rheol.* **1993**, *37*, 695-725.
- (8) Lauber, L.; Colombani, O.; Nicolai, T.; Chassenieux, C. *Macromolecules* **2016**, *49*, 7469-7477.